Low cost and compact nonlinear (SHG/TPE) laser scanning endoscope for bio-medical application

Jiayun Liu[a], Ken Choong Lim[a,b], Hao Li[a*], Hon Luen Seck[a], Xia Yu[a], Shaw Wei Kok[a], and Ying Zhang[a]

[a] Singapore Institute Of Manufacturing Technology, 71 Nanyang Drive, Singapore 638075;
[b] Nanyang Technological University, 50 Nanyang Avenue, Singapore 639798.

ABSTRACT

Two-photon fluorescence (TPE) and second harmonic generation (SHG) can been used to extract biological information from tissues at the molecular level, which is blind to traditional microscopes. Through these two image contrast mechanisms, a nonlinear laser scanning endoscope (NLSE) is able to image tissue cells and the extra cellular matrix (ECM) through a special fiber and miniaturized scanner without the requirement of poisonous chemical staining. Therefore, NLSE reserves high potential for in-vivo pathological study and disease diagnosis. However, the high cost and bulky size of a NLSE system has become one of the major issues preventing this technology from practical clinical operation. In this paper, we report a fiber laser based multi-modality NLSE system with compact size and low cost, ideal for in-vivo applications in clinical environments. The demonstration of the developed NLSE nonlinear imaging capability on different bio-structures in liver, retina and skin are also presented.

Keywords: Second-harmonic generation, Two-photon fluorescence, Ultrafast fiber laser, Endoscopy

1. INTRODUCTION

Nonlinear laser scanning imaging (NLSI) techniques have recently been a promising method for non-invasive imaging on biological tissues targeted at in-vivo disease diagnosis applications. Due to their high molecular imaging specificity, TPE and SHG have been applied to deduce pathological irregularities beneath the skin in various types of diseases diagnosis, without introducing any fluorescence dye which is toxic to tissues[1-5]. However, most research on nonlinear optical imaging techniques are still focused on demonstration of principle in the laboratory rather than real clinical applications. One of the major reasons for this is that most available nonlinear laser scanning microscope systems rely on a Ti:sapphire laser to provide high power optical pulses for nonlinear signal generation. However, the complexity of a Ti:sapphire laser requires frequent maintenance and can only be operated by an optical specialist with a high level of technical expertise. Furthermore, a large footprint and high cost prevents nonlinear optical imaging systems from commercial usage. Lastly, a NLSI system implemented in a bulky microscope configuration cannot be used for endoscopic diseases diagnosis of inner organs.

An endoscopic NLSI system will greatly expand the application of nonlinear optical imaging techniques in medical, biology and life-science industries. However, most currently available NLSE systems can only offer TPE imaging capability. Currently, several SHG endoscopic imaging systems have been proposed, however only specific samples with ultra-high SHG emission intensities such as mouse tails are able to be imaged. In this paper, we demonstrate a high sensitivity NLSE system capable of simultaneously obtaining TPE and SHG images from multiple biopsy and in-vitro tissues including liver, retina and skin. Notably, by using high throughput optical designs, we can achieve high sensitivity SHG and TPE imaging with a cheap and low power fiber laser source rather than a Ti:sapphire laser. To the best of our knowledge, this is the first endoscopy system, which have successfully adopted a fiber laser source for nonlinear optical imaging. The resulting system has a compact size, low cost and is maintenance free. These features make it very attractive for clinical applications.

*hli@simtech.a-star.edu.sg, Hp: 65-90407316; Fax: 65-67916377

Endoscopic Microscopy X; and Optical Techniques in Pulmonary Medicine II, edited by Melissa J. Suter, Stephen Lam, Matthew Brenner, Guillermo J. Tearney, Thomas D. Wang, Proc. of SPIE Vol. 9304, 93041K · © 2015 SPIE · CCC code: 1605-7422/15/$18 · doi: 10.1117/12.2078809

2. ENDOSCOPE SYSTEM DESIGN

2.1 Experimental Setup

The schematic of the developed NLSE system is depicted in Fig. 1. The whole footprint the system is about 100x40x25cm. A compact ultrafast fiber laser (Toptica FemtoFiber pro) was used to provide optical pulses with 100 fs time duration at 80 MHz repetition rate. The maximum average power at the output of the laser was about 120 mW.

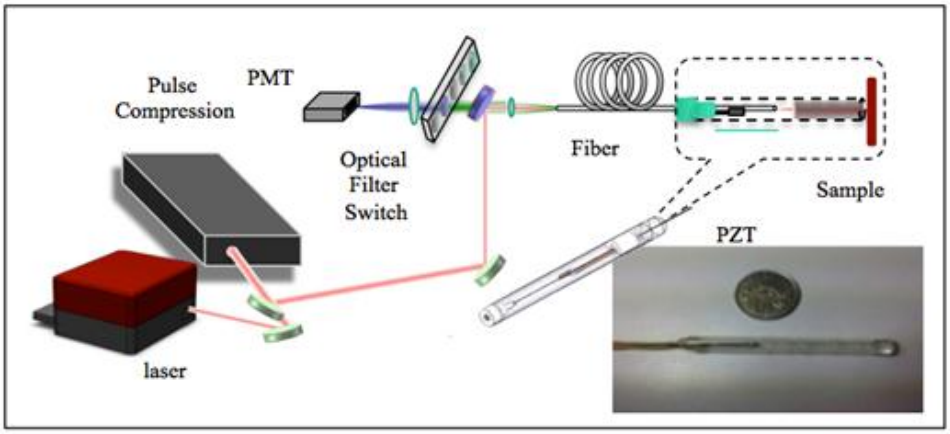

Figure 1. Schematic of nonlinear optical endoscope setup.

A 1-m long double cladding fiber (DCF) with an inner core diameter of 9 μm and a cladding diameter of 105 μm was used to deliver illumination laser light to the sample as well as transmit the excited SHG and TPE signal back to the detector. At the distal end of the fiber, a rigid endoscopic probe (inset of Fig. 1) with a diameter of 4 mm and a length of 20 mm was used to focus laser light onto the sample surface. The rigid probe contains a GRIN lens (GT-MO-080-018-810, GrinTech GmbH) and a miniaturized fiber actuator connected to the end of the DCF fiber. The fiber actuator contains two bimorphs with lengths of 3 mm and 9 mm. The 3 mm bimorph was driven by a RF signal with a frequency of 150 Hz and vibrates in resonant mode along the horizontal direction. The 9 mm bimorph was driven by an electronic signal and vibrates along the vertical direction. The two bimorphs were connected orthogonal with each other at one end. They were used to implement raster scanning of the DCF fiber end. To avoid cross-coupling between the horizontal and vertical axes, the two bimorphs were coaxially mounted along their axis of symmetry along the largest dimension. With this design, coupling between the two bimorphs was suppressed and rectangular shape field of view can be achieved. A 1 MHz clock signal was used to synchronize the motion of two bimorphs and trigger the photo detector to perform data collection. A field of view of 100x100 μm was achieved by applying 6 V and 14 V (peak to peak voltage) signals on the resonant and non-resonant bimorphs respectively.

The frame rate of the system was measured to be 0.3 frame/s at 512 × 512 pixel resolution. The maximum frame rate was limited by the response speed of the photo multiplier tube (PMT) used in the system, which is 200 kHz. A collimator was attached at the end of the DCF. On one hand, it couples the excitation laser into the DCF core along the forward direction. On the other hand, this collimator collects the SHG and TPE signals from the cladding of the fiber in the backward direction and guides it to the PMT for detection.

To efficiently excite a SHG and TPE signal, the pulse width of the laser before reaching the sample is expected to be as narrow as possible. However, the group delay dispersion (GDD) induced by a 1 m long double cladding fiber (DCF) was approximately 64,000 fs^2. With such a high GDD, a 100 fs input pulse will be stretched to about 2 ps as shown in Fig. 3, rendering SHG or TPE imaging impossible[6]. To compensate for the huge dispersion induced by the DCF fiber, a dispersion compensation module (DCM) was integrated into our system.

Due to the limited optical power budget of the optical fiber laser used in the system, we designed a prism based DCM module with a power transmission of 90%. This is much higher than the 65% transmission (single reflection) of optical grating pairs used in Ti:sapphire laser based NLSI systems[7]. Chirped mirrors also can be used for GDD compensation and their reflectivity can be as high as 99%. However, one reflection from a chirped mirror can only

induce about -60 fs^2 GDD [8]. To compensate for the GDD induced by 1 m of DCF, roughly 1060 reflections is need which leads to a 99.8% power loss. In comparison, using our prism-based DCM, a maximum GDD of up to 80,000 fs^2 with a dynamic range of 30,000 fs^2 can be induced into the laser pulse before entering the fiber. The overall optical throughput of our system before entering the fiber was measured at 75%. The major optical loss was due to the mirrors and lens used in the system for laser steering. The laser was coupled into the core of the DCF by a fiber collimator. Through carefully adjusting the incident angle of the laser with respect to the fiber collimator, we achieved a maximum power (core mode only) output of approximately 50 mW at the other end of DCF.

Light propagation in the cladding mode of the DCF fiber cannot be focused by the GRIN lens and has no contribution to SHG and TPE excitation. Therefore, the core to cladding coupling ratio is critical for implementing nonlinear optical imaging through an optical fiber. High core to cladding coupling ratio was achieved by adjusting the incident laser beam's angle and imaging the output end of the fiber which is shown in Figure 2(a). Misalignment of laser into DCF can be easily detected by the low coupling ratio between the core and cladding as shown in Figure 2(b).

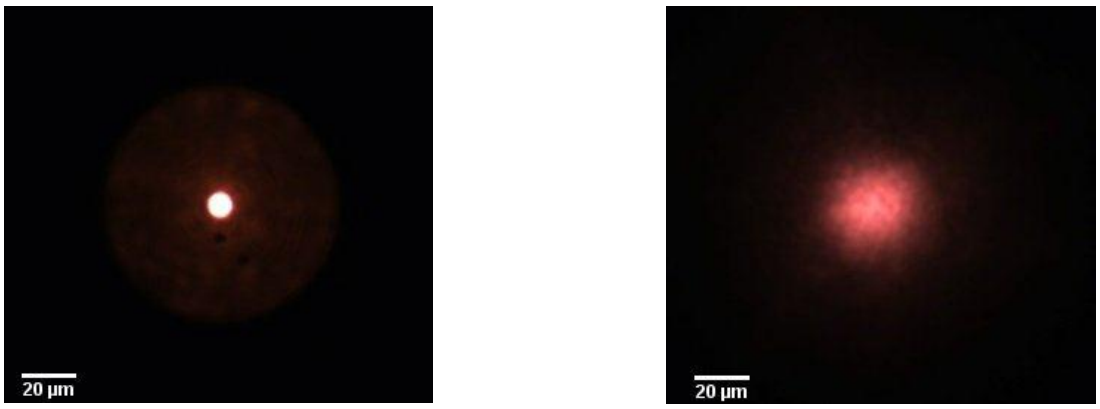

(a) (b)

Figure 2. Imaging of laser spot at the DCF fiber's end using a CCD camera. (a) high core to cladding coupling ratio and (b) low core to cladding coupling ratio due to misalignment.

2.2 Pulse Compression Module Performance

Frequency Resolved Optical Gating (FROG) was used to characterize the temporal profile of the laser pulse at different locations along the optical path. The pulse width at the fiber laser output was 100 fs and its temporal profile and FROG trace are shown in Figure 3 (a) and (b). The temporal profile and FROG trace of the laser pulse before and after the DCF fiber without DCM are shown in Figure 3 (c) and (d). By inserting the DCM module into the optical path, a 160 fs transform limited pulse was achieved at the fiber end as shown in Figure 3(e) and (f). The spectral narrowing of the laser pulse is due to the self-phase modulation in the fiber with a negative chirped input pulse[6].

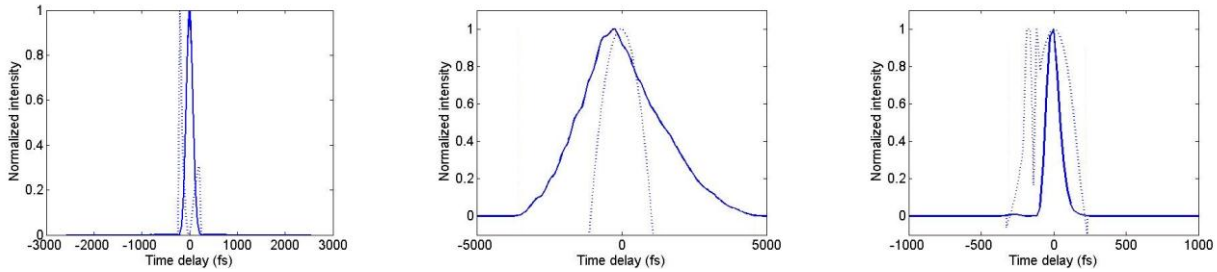

(a) (b) (c)

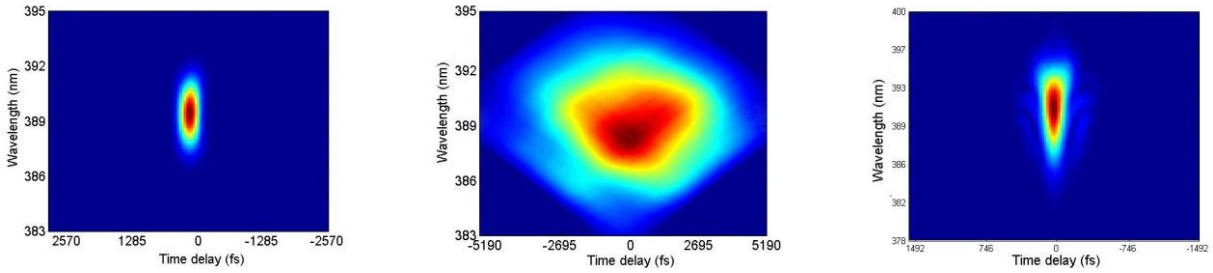

Figure 3. FROG measurement of pulse profile at the fiber laser output (a,d),after 1m DCF fiber (b,e), after DCM and 1m DCF fiber (c,f). (a-c) show the temporal profile and (d-f) show the FORG traces obtained.

3. OPTICAL PERFORMANCE CHARACTERIZATION

To determine detailed system specifications, polystyrene spheres of 1 μm diameter was mixed with diluted Rhodamine 6G dye for fluorescence imaging. The images were then processed to get the point spread function (PSF) of the system. Fig. 4 shows the spatial distribution of fluorescence intensity obtained from an isolated polystyrene sphere. From the figure, the lateral resolution is estimated to be about 1.6 μm.

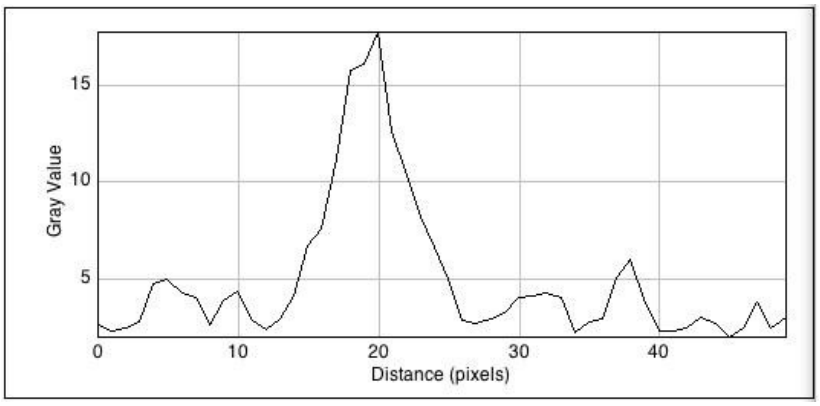

Figure 4. Spatial distribution of fluorescence intensity obtained from a polystyrene sphere dyed with Rohdamine 6G.

To evaluate the axial resolution of the system, Z-stack scanning with a step size of 1 μm was performed on the polystyrene sphere sample. A 3D model of the obtained data is shown in Fig. 5. The spherical features (inside the circle) was observable within 5 adjacent stacks. Therefore, the system axial resolution is estimated to be 5 μm.

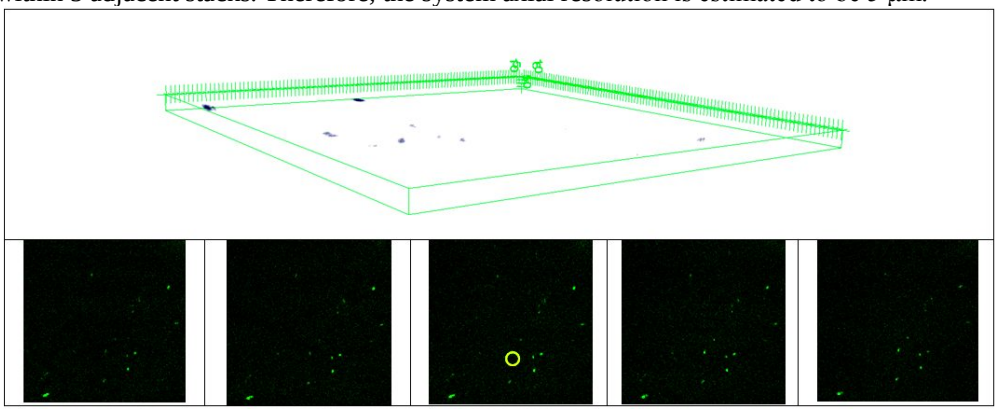

Figure 5. System axial resolution measurement. Upper panel: 3D model of polystyrene spheres. Lower panel: Z-stacks of 3D model with a step size of 1 μm.

4. TISSUE IMAGING

Several biopsy tissues including mouse liver, retina and swine skin were used to demonstrate the tissue imaging capability of the developed NSLE system. All these tissues were not stained and were mounted on a translational stage. The tissue samples were positioned at the focal plane of the GRIN lens. SHG and TPE signals emitted from the tissues were collected via the GRIN lens in the rigid endoscopic probe and were transmitted through the DCF cladding to the PMT. Two bandpass filters with central wavelengths at 390 nm (Semrock FF01-390/18-25) and 550nm (Semrock FF01-550/80-25) were inserted in front of the PMT to select the SHG and TPE signals respectively. Fig. 6 shows the nonlinear images obtained by using the developed NLSE system. The SHG and TPE signals are encoded in green and red colors respectively. In Fig. 6 (a), hepatic cells can be clearly recognized in the TPE image of a mouse liver tissue. Collagen fibril structures with strong SHG emission can also be observed around the blood vessels in Fig. 6 (a). Due to the forward propagating nature of the generated SHG signals, we observe much weaker SHG signals compared to TPE signals from the liver sample. Fig. 6 (b) shows the nonlinear image of retina pigment epithelium tissues, which exhibit strong TPE signals but no SHG signals. Fig. 6 (c) shows the nonlinear imaging of swine skin. Due to the thick layer of collagen at the skin epidermis, strong SHG signals can be detected but no TPE signals were observed. These images demonstrate the tissue imaging capability of the developed compact and low cost NLSI endoscope system. The quality of the images obtained using this system is estimated to be higher than conventional NLSI endoscope systems and comparable to those obtained by nonlinear microscope systems in epi mode, although they are equipped with higher power Ti:sapphire lasers[9].

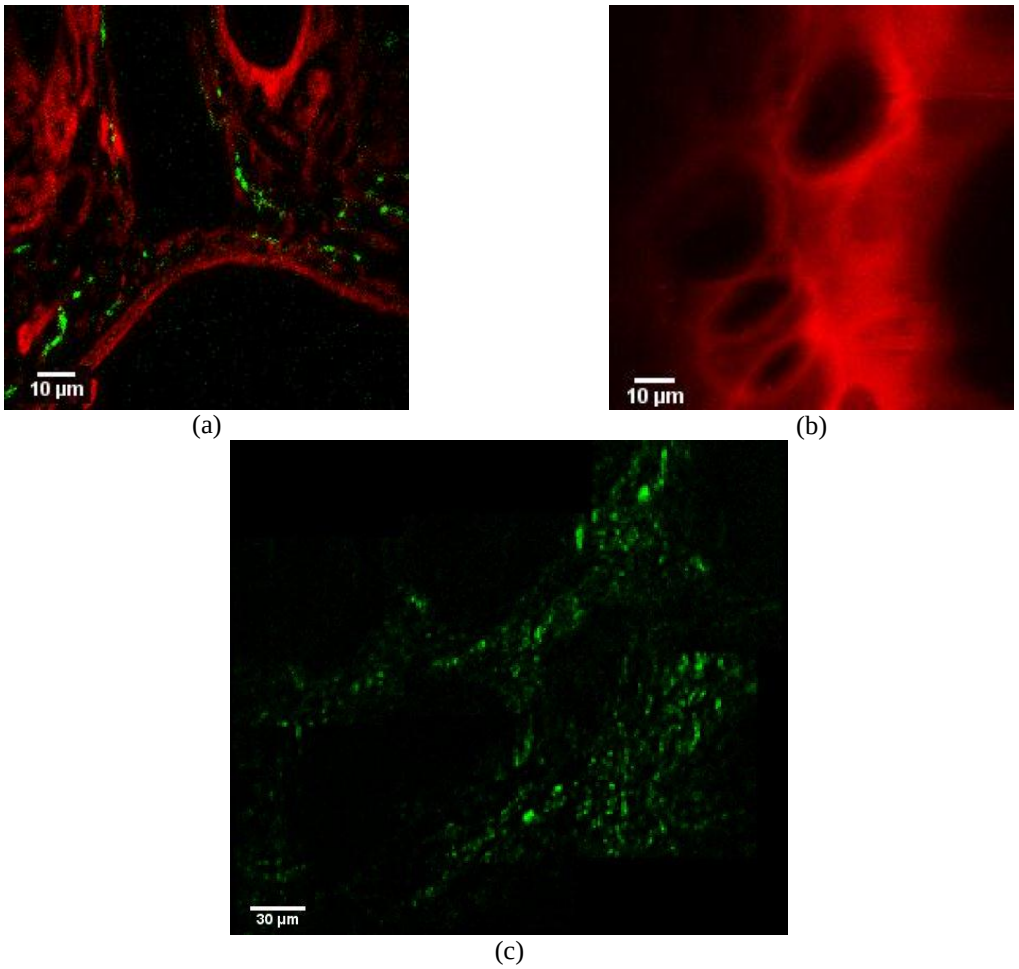

(a) (b)

(c)

Figure 6. SHG and TPE images of biopsy mouse liver (a); retina (b); swine skin (c). The SHG signals and TPE signals are encoded in green and red color respectively.

5. CONCLUSION

A nonlinear endoscope system able to simultaneously image TPE and SHG has been developed. In the system, a cheap and low power fiber laser source was used to replace the bulky and expensive Ti:sapphire laser. By using high throughput optical designs, nonlinear imaging capability (SHG/TPE) with high sensitivity has been achieved and demonstrated in epi mode on multiple biopsy and in-vitro tissues including liver, retina and skin. To the best of our knowledge, it is the first endoscope system which successfully adopted a fiber laser source for nonlinear optical imaging. The resulting reduction of system size, cost and maintenance requirements make the developed NLSE system attractive for clinical applications.

ACKNOWLEDGEMENTS

We wish to acknowledge our collaborator Dr. Dean Tai Chi Shang and Dr. Gideon Ho from HistoIndex Pte. Ltd. for technical discussion and suggestion.

REFERENCES

[1] L. Wu, L. Fu, A. Jain, T. Nishida, M. Gu, and H. Xie, "An Endoscopic Nonlinear Optical Imaging Probe Based on 2-D Micromirror," LEOS IEEE Lasers and Electro-Optics Society Annual Meeting, 908-909 (2007).

[2] M. Both, M. Vogel, O. Friedrich, F. V. Wegner, T. Künsting, R. H. A. Fink, and D. Uttenweiler, "Second harmonic imaging of intrinsic signals in muscle fibers in situ," Journal of Biomedical Optics, 9(5), 882-892 (2004).

[3] S. W. Chu, S. P. Tai, C. K. Sun, and C. H. Lin, "Selective imaging in second-harmonic-generation microscopy by polarization manipulation," Appl. Phys. Lett., 91(10), 103903 1-3, (2007).

[4] D. R. Rivera, C. M. Brown, D. G. Ouzounov, I. Pavlova, D. Kobat, W. W. Webb, and C. Xu, "Compact and flexible raster scanning multiphoton endoscope capable of imaging unstained tissue," Proc Natl Acad Sci USA, 108(43), 17598–17603, (2011).

[5] M. T. Myaing, D. J. MacDonald, and X. Li, "Fiber-optic scanning two-photon fluorescence endoscope," Opt. Lett., 31(8), 1076-1078, (2006).

[6] R. W. Boyd, [Nonlinear Optics (Second Edition)], Academic Press, UK, (2003).

[7] E. B. Treacy, "Optical pulse compression with diffraction gratings," IEEE J. Quantum Electron., 454-458, (1969).

[8] S. Chen, P. Gao, Y. Zhao, Y. Wang, Z. Fang, Y. Leng, and J. Shao, "Thermal-dynamical analysis of blister formation in chirped mirror irradiated by single femtosecond lasers," Appl. Opt., 53(15), 3347-3354, (2014).

[9] H. Bao, A Boussioutas, R Jeremy, S Russell, and M Gu, "Second harmonic generation imaging via nonlinear endomicroscopy," Opt. express, 18(2), 1255-1260, (2010).